

University of Wollongong  
**Research Online**

---

Australian Institute for Innovative Materials -  
Papers

Australian Institute for Innovative Materials

---

1-1-2013

## A study of TiO<sub>2</sub> binder-free paste prepared for low temperature dye-sensitized solar cells

Jeremy H. Yune

*Australian Nuclear Science and Technology Organisation (ANSTO)*

Inna Karatchevtseva

*Australian Nuclear Science and Technology Organisation (ANSTO)*

Gerri Triani

*Australian Nuclear Science And Technology Organisation (ANSTO)*

Klaudia Wagner

*University of Wollongong, kwagner@uow.edu.au*

David Officer

*University of Wollongong, davido@uow.edu.au*

Follow this and additional works at: <https://ro.uow.edu.au/aiimpapers>



Part of the [Engineering Commons](#), and the [Physical Sciences and Mathematics Commons](#)

---

### Recommended Citation

Yune, Jeremy H.; Karatchevtseva, Inna; Triani, Gerri; Wagner, Klaudia; and Officer, David, "A study of TiO<sub>2</sub> binder-free paste prepared for low temperature dye-sensitized solar cells" (2013). *Australian Institute for Innovative Materials - Papers*. 574.

<https://ro.uow.edu.au/aiimpapers/574>

Research Online is the open access institutional repository for the University of Wollongong. For further information contact the UOW Library: [research-pubs@uow.edu.au](mailto:research-pubs@uow.edu.au)

---

## A study of TiO<sub>2</sub> binder-free paste prepared for low temperature dye-sensitized solar cells

### Abstract

A binder-free titania paste was prepared by chemical modification of an acidic TiO<sub>2</sub> sol with ammonia. By varying the ammonia concentration, the viscosity of the acidic TiO<sub>2</sub> suspension increased, thereby allowing uniform films to be cast. The photoelectrochemical performance of TiO<sub>2</sub> electrodes, cast as single layers, was dependent on the thermal treatment cycle. Fourier transform infrared spectroscopy was used to characterize the extent of residual organics and found that acetates from the TiO<sub>2</sub> precursor preparation were retained within the electrode structure after thermal treatment at 150 °C. Electrodes of nominal thickness 4 μm produced an energy conversion efficiency as high as 5.4% using this simple thermal treatment.

### Keywords

temperature, dye, sensitized, solar, low, cells, paste, free, binder, tio<sub>2</sub>, study, prepared

### Disciplines

Engineering | Physical Sciences and Mathematics

### Publication Details

Yune, J. H., Karatchevtseva, I., Triani, G., Wagner, K. & Officer, D. (2013). A study of TiO<sub>2</sub> binder-free paste prepared for low temperature dye-sensitized solar cells. *Journal of Materials Research*, 28 (3), 488-496.

# A study of TiO<sub>2</sub> binder-free paste prepared for low temperature dye-sensitized solar cells

Jeremy H. Yune, Inna Karatchevtseva, and Gerri Triani<sup>a)</sup>

*Institute of Materials Engineering, Australian Nuclear Science and Technology Organisation (ANSTO), Lucas Heights, Menai, New South Wales 2234, Australia*

Klaudia Wagner and David Officer

*Intelligent Polymer Research Institute, University of Wollongong, Innovation Campus, Fairy Meadow, New South Wales 2519, Australia*

(Received 7 May 2012; accepted 16 October 2012)

A binder-free titania paste was prepared by chemical modification of an acidic TiO<sub>2</sub> sol with ammonia. By varying the ammonia concentration, the viscosity of the acidic TiO<sub>2</sub> suspension increased, thereby allowing uniform films to be cast. The photoelectrochemical performance of TiO<sub>2</sub> electrodes, cast as single layers, was dependent on the thermal treatment cycle. Fourier transform infrared spectroscopy was used to characterize the extent of residual organics and found that acetates from the TiO<sub>2</sub> precursor preparation were retained within the electrode structure after thermal treatment at 150 °C. Electrodes of nominal thickness 4 μm produced an energy conversion efficiency as high as 5.4% using this simple thermal treatment.

## I. INTRODUCTION

Since the pioneering work of O'Regan and Grätzel in 1991,<sup>1</sup> there has been great interest by the research community to understand the fundamental interactions of components (i.e., semiconductor oxide, sensitizer, and electrolyte) within the dye-sensitized solar cell (DSSC). This focus has led to many refinements in both materials and processes, which have improved the energy conversion efficiency of conventional DSSCs to 12.3%.<sup>2</sup> A prime area of development has been centered on the mesoporous TiO<sub>2</sub> architecture, which is used as high surface area electrodes for electron transport. TiO<sub>2</sub> electrodes for DSSC are typically prepared by coating with a viscous paste prepared with organic binders onto a conducting glass substrate, followed by thermal treatment at temperatures >400 °C to allow organic compound elimination and subsequent particle binding and adhesion to the substrate.<sup>3</sup>

Currently, a key driver in the commercialization of DSSCs is the preparation of robust TiO<sub>2</sub> electrodes at low temperature (≤150 °C). This reduction in process temperature opens up the possibility of using polymer substrates in continuous roll-to-roll processing. Several process methods have been explored in the preparation of low temperature electrodes. They include mechanical compression,<sup>4–9</sup> hydrothermal necking of

titanium salts,<sup>10–12</sup> ultraviolet (UV)–O<sub>3</sub> curing,<sup>13–15</sup> and microwave sintering.<sup>16,17</sup> Although the compression method in combination with UV–O<sub>3</sub> treatment has reported an efficiency of 7.6% on indium tin oxide (ITO)/polyethylene naphthalate (PEN), integration of such a process in DSSC device fabrication remains challenging.

Casting of films onto substrates is by far the preferred method of preparing electrodes for DSSC. However, additives for low temperature TiO<sub>2</sub> paste must provide adequate viscosity and volatility to produce uniform porous structures. An interesting method reported by Park et al.<sup>18,19</sup> utilizes a binder-free formulation by adding small quantities of ammonia solution into an acidic TiO<sub>2</sub> aqueous sol. Indeed, surface-mediated couples CH<sub>3</sub>COO<sup>−</sup>/NH<sub>4</sub><sup>+</sup> are formed within the slurry, which results in the reduction of the double layer repulsion between the particles; consequently, this induces TiO<sub>2</sub> particles to flocculate sufficiently to allow an increase in viscosity. This approach was successfully demonstrated by Park casting 4.2-μm-thick TiO<sub>2</sub> electrodes on ITO/glass yielding a maximum light to electrical energy conversion efficiency of 2.83% after heat treatment to 150 °C. Additional improvements were made by immersing low temperature TiO<sub>2</sub> films in a solution of TiCl<sub>4</sub> to assist binding between nanoparticulates, thereby increasing device efficiency from 2.83% to 4.18%.<sup>19</sup> Using a similar methodology, Zhang et al.<sup>20</sup> extended this approach by preparing a bimodal particle sized paste with a blend of P25 and 200-nm anatase particles with the addition of hydrothermal TiO<sub>2</sub> solution to improve interparticle connectivity. TiO<sub>2</sub> electrodes were treated

<sup>a)</sup>Address all correspondence to this author.

e-mail: gerry.triani@ansto.gov.au

DOI: 10.1557/jmr.2012.354

to 120 °C on ITO/polyethylene terephthalate (PET) to yield efficiencies up to 4.00%.

In recent studies of TiO<sub>2</sub> binder-free systems, Weerasinghe et al.<sup>21,22</sup> investigated the rheological behavior of a pure ethanolic or mixed ethanolic/water P25 (Degussa, Essen, Germany) paste prepared for polymer DSSC. TiO<sub>2</sub> suspensions were chemically modified by addition of either acidic or basic compounds or water to yield viscous slips. Their study found that both slurry rheology and interparticle connectivity influenced mechanical integrity and bonding to the polymeric substrate. Energy conversion efficiencies of 5% (under one sun illumination—100 mW/cm<sup>2</sup>) were reported after processing at 150 °C for 30 min.

In our study, a preparative method described by Park was investigated to establish the influence of ammonia on the viscosity and the binding of an aqueous TiO<sub>2</sub> colloidal suspension. Unlike Park, an equimolar ratio of acid to titanium alkoxide was used to prepare the TiO<sub>2</sub> colloidal suspension. This allows for minimal quantity of organics to be used in the subsequent paste. TiO<sub>2</sub> film thickness and post-treatment cycle were also examined to determine their effect on DSSC performance and electron lifetime. As a result of this investigation, adjustments to TiO<sub>2</sub> suspension viscosity allowed uniform electrodes to be cast onto glass. Electrodes with a nominal thickness of 4.2 μm produced an energy conversion efficiency of 5.44% after thermal treatment at 150 °C. Moreover, the stability of this TiO<sub>2</sub> formulation was investigated over a 9-month period to establish the effects of paste aging on the resultant TiO<sub>2</sub> electrode structure and its performance in DSSC devices.

## II. MATERIALS AND METHODS

### A. Preparation of binder-free TiO<sub>2</sub> paste

TiO<sub>2</sub> solutions were prepared by a method reported by Karatchevtseva et al.<sup>23</sup> Briefly, 85 mL of titanium(IV) isopropoxide was mixed with 17.4 g of glacial acetic acid (1:1 molar ratio) in a glove box under inert conditions and vigorous stirring. This solution was slowly added via a dropping funnel to 512 g of H<sub>2</sub>O under vigorous stirring for 10 min at room temperature followed by the addition of 5 mL of nitric acid (concentration 69%), used as a peptization agent.<sup>24,25</sup> The reaction mixture was heated at 80 °C under vigorous stirring for 8 h. TiO<sub>2</sub> sol was converted into highly crystalline anatase via a hydrothermal procedure by introducing 150 g of TiO<sub>2</sub> sol into a 200 mL titanium autoclave heated to 240 °C, which was controlled by ramping at 2 °C/min and held at temperature for 14 h. An aqueous TiO<sub>2</sub> suspension of anatase with uniform particle size distribution was collected after ultrasonication for 15 min followed by centrifugal separation at a rotation speed of 3000 min<sup>-1</sup> for 15 min.

Binder-free TiO<sub>2</sub> paste was prepared by adding a known quantity of 10 M ammonia solution, diluted from 25% conc.

NH<sub>4</sub>OH solution (13 M) to 5 g of acidic anatase TiO<sub>2</sub> colloidal solution. This paste was concentrated by rotavapor to 12.5% weight of TiO<sub>2</sub> and confirmed by thermogravimetric analysis. A range of paste was prepared by varying the amount of NH<sub>4</sub>OH from 0.5 to 5 wt% with respect to TiO<sub>2</sub>.

TiO<sub>2</sub> films were prepared on either microscope soda lime glass slides or indium-doped tin oxide coated on glass substrates (Asahi, Tokyo, Japan, sheet resistance:  $R_s \leq 8 \Omega/\text{sq}$ ) using the doctor blade technique. The TiO<sub>2</sub> films were first air dried for 30 min and then heat treated on a hot plate at 150 °C for either 15 min, 2 h, or 24 h and designated accordingly, before assembly in devices.

### B. DSSC preparation

TiO<sub>2</sub> films with an effective area of 5 by 5 mm were further treated for 2 h at 120 °C on a hot plate, to remove most of physisorbed water, and immersed while hot into 0.3 mM anhydrous cis-diisothiocyanato-bis(2,2'-bipyridyl-4,4'-dicarboxylato) ruthenium(II) bis(tetrabutylammonium) (N719 dye purchased from Solaronix SA Ltd., Aubonne, Switzerland) solution in acetonitrile/tert-butyl alcohol (1/1) for 22 h. The sensitized TiO<sub>2</sub> electrode was sandwiched with a Pt-sputtered (~30 nm thickness) ITO-glass counter electrodes (Delta Technologies, Loveland, CO,  $R_s \sim 10 \Omega/\text{sq}$ ) spaced with a 25 μm Surlyn sealant. An electrolyte solution comprising of 0.6 M 1,2-dimethyl-3-propylimidazolium iodide, 0.5 M 4-tert-butylpyridine, 0.1 M LiI, and 0.05 M I<sub>2</sub> in a solvent mixture of 85:15 acetonitrile/valeronitrile was injected between the electrodes through a hole in the counter electrode by a vacuum-filling procedure. Triplicate samples were prepared for every condition investigated.

### C. Characterization

The effect of ammonia concentration on TiO<sub>2</sub> suspension viscosity was investigated using a Haake RS150 RheoStress rheometer (Thermo Scientific Inc., Karlsruhe, Germany) with cone (60 mm and 1°) and plate geometry maintained at 25 °C. Samples containing different quantities of ammonia were measured over a shear rate range of 1–500 s<sup>-1</sup> yielding plots of the shear stress and viscosity as a function of shear rate. The viscosity of these samples is reported at a shear rate of 2.5 s<sup>-1</sup> to compare with experimental data reported in the literature.

The thickness of both air-dried and thermally treated TiO<sub>2</sub> films on glass were measured using the Alpha-Step IQ Surface Profiler (KLA-Tencor, Milpitas, CA). Further, measurements of film transmittance were recorded by UV-Vis spectroscopy on a Perkin Elmer Lambda 35 UV-Vis spectrometer (Waltham, MA).

TiO<sub>2</sub> interparticle connectivity and specific surface area of air-dried and thermally treated electrodes were measured by Brunauer-Emmett-Teller (BET) nitrogen adsorption method. Thick cast films were removed from their

substrates by scratching and placing contents into glass bulbs for measurement. Nitrogen adsorption isotherms at 77 K were measured on a Quantachrome AutoSorb iQ volumetric adsorption analyzer (Boynton Beach, FL).

Scanning electron microscopy (SEM) provided a comparative study of TiO<sub>2</sub> film morphology. Samples were examined by field emission SEM (Zeiss Supra 55VP, Carl Zeiss, Berlin, Germany) operating at an accelerating voltage of 10 kV. Films were mounted on a conductive carbon adhesive, and approximately 30 Å thick platinum was evaporated onto the surface to prevent charging.

Fourier transform infrared spectroscopy (FTIR) spectra were obtained on a Nicolet Nexus 8700 FTIR spectrometer (Thermo Electron Corporation, Madison, WI). Both dried and thermally treated films were measured using the Smart iTR™ (Thermo Scientific Inc., West Palm Beach, FL) sampling accessory equipped with a single bounce diamond attenuated total reflectance crystal. Spectra were recorded in absorbance mode by averaging 32 scans with a nominal resolution of 4 cm<sup>-1</sup>.

Current–voltage curves were recorded using a Keithley 2400 instrument (Keithley Instruments Inc., Cleveland, OH) by illuminating the DSSCs with a simulated 100 mW/cm<sup>2</sup> AM 1.5 light source (Oriol), calibrated using a certified Si diode equipped with a KG5 filter (Peccell Technologies Inc., Kanagawa, Japan). The device area was masked with black paint defining an aperture slightly larger than the active area.<sup>26</sup> The short-circuit current response of the devices was recorded in 5-nm steps using the Keithley 2400 unit and referenced to the response of a calibrated silicon diode (Peccell).

Electrochemical impedance spectroscopy (EIS) measurements were recorded by illuminating the DSSCs with 100 mW/cm<sup>2</sup>. A calibrated AM 1.5 illumination at open-circuit conditions between 0.1 Hz and 100 kHz with an AC amplitude of 10 mV using a Gamry Reference 600 instrument (Garry Instruments, Warminster, PA). Spectra were analyzed and fitted using ZView version 3.0.

### III. RESULTS AND DISCUSSION

#### A. Synthesis of TiO<sub>2</sub> colloid

A TiO<sub>2</sub> colloid was prepared from an equimolar ratio of acetic acid to titanium alkoxide. The introduction of acetic acid to titanium alkoxide allows for chemical modification of the precursor, thus permitting the control of hydrolysis and condensation reaction rates. Under this synthesis, the coordination number of Ti increases from 4 to 6 and oligomeric species are formed.<sup>27</sup> During hydrolysis of these intermediate acetoalkoxy species Ti(OR)<sub>x</sub>(CH<sub>3</sub>COO)<sub>y</sub>, alkoxy groups are removed first, whereas acetate ligands are more difficult to react and can remain in the titanium sol up to 300 °C, as reported by Doeuff. In this study, 1:1 acetic acid to titanium ratio was used to slow down condensation reaction rate to produce stable nanosized titania

colloid. Additionally, the amount of organic component was designed to be minimal to ensure removal during thermal treatment, where organics can affect electron transport.<sup>13</sup>

#### B. Paste and film characterization

It is well known that TiO<sub>2</sub> electrodes characteristics, such as film porosity, particle size, and crystallinity, can influence the overall DSSC device performance and that fine tuning of TiO<sub>2</sub> microstructure can affect the mechanical, optical, and electrical properties. Equally, the chemical composition of the titania paste and, more specifically, the weight percentage of TiO<sub>2</sub><sup>28</sup> are additional factors that influence on the electrode microstructure.

The initial paste prepared in this study was kept constant at 12.5 wt% of TiO<sub>2</sub> as described in Sec. II. A. A calculated quantity of ammonia was added to increase the viscosity of the acidic TiO<sub>2</sub> suspension. Pastes were designated as *x*-TiO<sub>2</sub>, where *x* is the weight ratio of NH<sub>4</sub>OH:TiO<sub>2</sub>. TiO<sub>2</sub> pastes prepared in this study are given in Table I, along with molar ratios of all constituents including acetic acid and water.

Upon addition of ammonia to the acidic TiO<sub>2</sub> colloid, the viscosity of the resulting mixture changed dramatically as shown in Fig. 1. At 0.5-TiO<sub>2</sub>, the paste viscosity is approximately at the instrument limit of sensitivity, which indicates that this amount of NH<sub>4</sub>OH does not impart an effect on the slurry. Paste viscosity reaches a maximum of 4 Pa·s for the 1-TiO<sub>2</sub> paste and then gradually decreases to around 0.4 Pa·s for the 5-TiO<sub>2</sub> paste, where an excess of NH<sub>4</sub>OH induces flocculation and separation of the particles from the slurry. A similar trend was observed for all pastes at different shear rates with plots of viscosity as a function of shear rates shown in the Supplementary section, Fig. S1 and Table SI.

The use of ammonia solution to increase the viscosity of TiO<sub>2</sub> suspension was originally reported by Park et al.<sup>18</sup> They attributed this effect to particle–particle interaction being induced by a reduction in the double layer interface. This results from an increase of ion concentration rather than an effect of pH associated with the isoelectric point of titania. Therefore, positively charged TiO<sub>2</sub> particles are held together by the CH<sub>3</sub>COO<sup>-</sup> and NH<sub>4</sub><sup>+</sup> ions through van der Waals attraction. In Park's study, the TiO<sub>2</sub> suspension was prepared using an excess

TABLE I. Paste composition with 12.5 wt% TiO<sub>2</sub>.

Paste ID	NH <sub>4</sub> OH/TiO <sub>2</sub> weight ratio, %	TiO <sub>2</sub> :CH <sub>3</sub> COOH:NH <sub>4</sub> OH:H <sub>2</sub> O molar ratio
0.5-TiO <sub>2</sub>	0.5	1:1:0.012:31.0
1-TiO <sub>2</sub>	1	1:1:0.023:31.0
2-TiO <sub>2</sub>	2	1:1:0.045:31.0
3.7-TiO <sub>2</sub>	3.7	1:1:0.084:30.9
5.0-TiO <sub>2</sub>	5.0	1:1:0.11:30.8

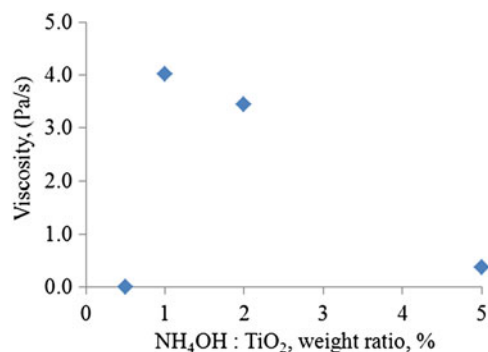


FIG. 1. Viscosity of the  $x$ -TiO<sub>2</sub> paste as a function of NH<sub>4</sub>OH:TiO<sub>2</sub> weight ratio at 2.5 s<sup>-1</sup> shear rate.

molar ratio of acetic acid. As a result, viscosity of paste reached a maximum at ~5 wt% of ammonia (NH<sub>3</sub>/TiO<sub>2</sub>) concentration. Beyond this maximum, the decline in viscosity was due to a dilution effect.

In our study, the TiO<sub>2</sub> content was kept constant in the final paste, and therefore, no dilution effect took place, with pH of all slurries being below 4; however, the maximum viscosity was observed at 1 wt% (NH<sub>3</sub>/TiO<sub>2</sub>) concentration. This difference can be explained by the fact that our TiO<sub>2</sub> colloid synthesis utilizes significantly smaller quantities of acetic acid, CH<sub>3</sub>COO<sup>-</sup>/TiO<sub>2</sub> molar ratio ~1, in comparison to a ratio of 10:1 of acetic acid to titania used by Park et al.<sup>18</sup>

Titania films were deposited on glass substrates using the doctor blading technique followed by heat treatment at 150 °C for 15 min. Under optical imaging, no particle aggregation was visibly detected for both 0.5-TiO<sub>2</sub> and 1-TiO<sub>2</sub> films. However, while the 1-TiO<sub>2</sub> film was uniform and continuous, the 0.5-TiO<sub>2</sub> film appeared to be uneven, presumably due to a low viscosity of the 0.5-TiO<sub>2</sub> paste. Further, there was noticeable particle aggregation in 2-TiO<sub>2</sub> and 3.7-TiO<sub>2</sub> films. Small cracks were also evident, emanating from the aggregates.

Figure 2 shows the transmittance patterns of TiO<sub>2</sub> electrodes prepared with the equivalent thickness in the UV-Vis region. The transmittance plot for the 0.5-TiO<sub>2</sub> composition is not shown since the resulting film quality was inconsistent.

At 633 nm, the transmittance of 1-TiO<sub>2</sub> film is approximately 79%. The trend decreases to 47% and 43% for 2-TiO<sub>2</sub> and 3.7-TiO<sub>2</sub> films, respectively. The decrease in transmittance is believed to be due to particle aggregation in these films as noted in optical imaging. Thus, based on the assessment of this property, a composition based on 1-TiO<sub>2</sub> was selected for subsequent experimental work.

### C. Film post-treatment

A key challenge for low temperature TiO<sub>2</sub> electrodes prepared from paste is to ensure that particle-to-particle connectivity and bonding to the substrate permit effective

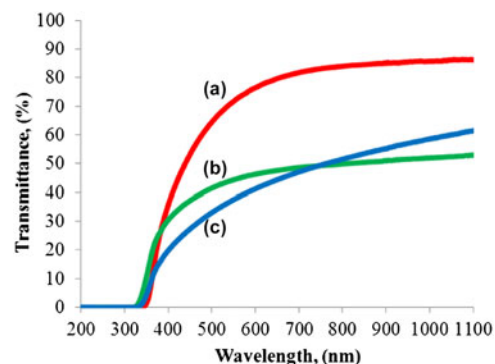


FIG. 2. The transmittance of the (a) 1-TiO<sub>2</sub>, (b) 2-TiO<sub>2</sub>, and (c) 3.7-TiO<sub>2</sub> films in the UV-Vis region. Films' thickness was 3 μm.

electron transport. If polymer substrates are to replace glass, soft thermal treatment procedures are required with the temperature not to exceed 150 °C. Postprocessing of TiO<sub>2</sub> electrodes that meet this criterion could be a limiting factor for DSSC efficiency, which makes the successful development of binder-free systems and their subsequent process treatments particularly important.

Figure 3 shows SEM images of titania films prepared using the 1-TiO<sub>2</sub> paste followed by different thermal treatment conditions. The morphology of TiO<sub>2</sub> film produced without the post-treatment [Fig. 3(a)] appears to be porous and rather uniform with well-dispersed nanoparticles seen throughout the film. Very little difference could be seen in the electrode microstructure thermally treated for 15 min at 150 °C, Fig. 3(b). Thermal treatment for 2 or 24 h at 150 °C resulted in slightly more compact film structures as observed in Figs. 3(c) and 3(d) where well interconnected particles are evident.

In addition to microstructural investigation, gas sorption analysis was used to assess changes that occurred to electrode films after thermal treatment. Nitrogen adsorption-desorption isotherms for both as-prepared and thermally treated TiO<sub>2</sub> films are provided in the Supplementary section, Fig. S2. They have been designated as type IV isotherms using the IUPAC classification scheme.<sup>29</sup> All isotherms exhibited a narrow type H1 hysteresis loop over the relative pressure range 0.80–1.0, associated with the capillary condensation in mesopores.

The BET surface area for as-cast (not treated) TiO<sub>2</sub> film was 86.5 m<sup>2</sup>/g. After thermal treatment at 150 °C for 15 min, the surface area increased slightly to 89.0 m<sup>2</sup>/g, which is due to the elimination of residual water and organic components from the film structure. Thermal treatment at 2 and 24 h has resulted in slight reduction of specific surface area to 85.2 and 85.3 m<sup>2</sup>/g, respectively. This suggests that the reduction in surface area could be a result of greater nanoparticles interconnectivity and, thus, more compact film morphology even though the pore size for all electrodes are equivalent [i.e., 13.1–13.2 nm (4 V/A)].

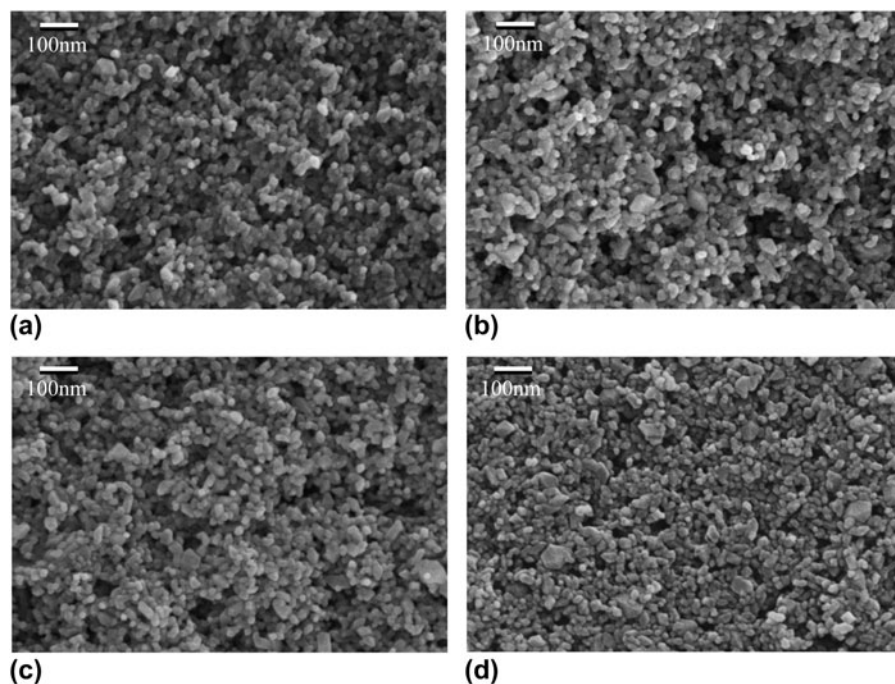


FIG. 3. SEM images of TiO<sub>2</sub> films prepared from 1-TiO<sub>2</sub> paste followed by: (a) no treatment; (b) 15 min at 150 °C; (c) 2 h at 150 °C; and (d) 24 h at 150 °C.

The presence of residual organics in the TiO<sub>2</sub> film structure is generally undesirable as it can reduce the photovoltaic properties of the TiO<sub>2</sub> electrode.<sup>13–15</sup> The removal of organics was monitored by the infrared spectroscopy. Typical FTIR spectra of as-prepared and thermally treated films are shown in Fig. 4.

Several common infrared (IR) adsorption bands were observed in each sample. First, the broad band below 800 cm<sup>-1</sup> is due to the formation of an extensive inorganic Ti–O–Ti network. The broad peak centered at 1633 cm<sup>-1</sup> is due to a combination of OH deformation and COO<sup>-</sup> asymmetric stretching vibrations.<sup>30</sup> In addition, the O–H stretching vibration was observed in the region ~3500–3000 cm<sup>-1</sup>. These OH bands originated from hydroxyl groups located on the titania surface that were retained in the structure after 24 h at 150 °C.

There is an additional broad peak in the IR patterns of both air-dried TiO<sub>2</sub> film and thermally treated electrodes at either 15 min or 2 h [Figs. 4(a)–4(c)]. This signature is characterized by several peaks located around 1435–1335 cm<sup>-1</sup>, which are assigned to the symmetric stretching vibration of COO<sup>-</sup> in carboxylic acid salt, which was a product of the neutralization between CH<sub>3</sub>COOH and NH<sub>4</sub>OH. The appearance of these specific peaks is typical for a salt of carboxylic acid. This broad peak became diffuse in the film treated at 150 °C for 24 h [Fig. 4(d)] and completely disappears after 30 min at 450 °C treatment [Fig. 4(e)]. Therefore, thermal treatment at relatively low temperature ~150 °C even for a long time (24 h) is not sufficient to remove all organic from the TiO<sub>2</sub> structure.

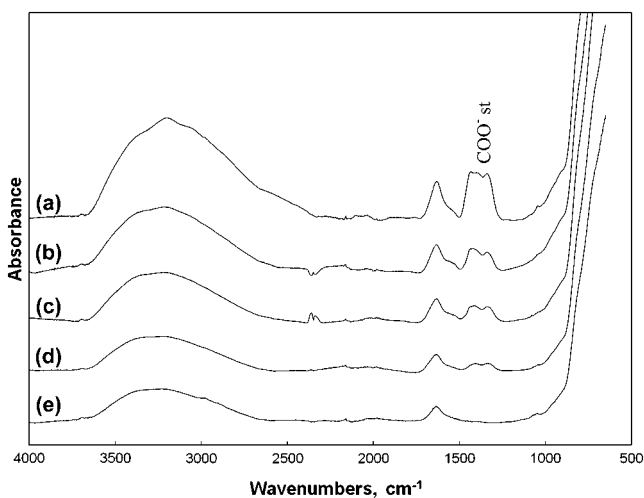


FIG. 4. FTIR spectra of TiO<sub>2</sub> electrodes prepared from 1-TiO<sub>2</sub> paste: (a) no treatment; (b) 15 min at 150 °C; (c) 2 h at 150 °C; (d) 24 h at 150 °C, and (e) 30 min at 450 °C.

#### D. DSSC performance

TiO<sub>2</sub> electrodes were prepared from 1-TiO<sub>2</sub> paste on indium-doped tin oxide substrates by doctor blading single or multiple casting to achieve TiO<sub>2</sub> film thickness between 2.5 and 7.7 μm. The photoelectrochemical properties of these electrodes were investigated as a function of TiO<sub>2</sub> thickness and thermal treatment cycle by preparing devices using N719 dye. The photovoltaic performance is summarized in Table II.

The overall efficiency ( $\eta$ ) is a percentage of solar energy irradiating onto the DSSC device, which is converted into electrical energy given by the equation below:

$$\eta = \frac{I_{SC} V_{OC} FF}{I_S},$$

where  $I_{SC}$  is the short-circuit current produced when the voltage and load resistance are zero,  $V_{OC}$  is the open-circuit voltage when the current is zero at infinite resistance, FF is the fill factor relating to a measure of the match between voltage at maximum power and  $V_{OC}$ , and  $I_S$  is the intensity of the incident light ( $I_S = 100 \text{ W/m}^2$ ).

At an equivalent TiO<sub>2</sub> film thickness and thermal processing conditions, the overall performance of DSSC prepared in this study was, in some cases, approximately 76% higher than devices reported by Park et al.<sup>18</sup> One plausible explanation for such a significant increase in the overall efficiency of the TiO<sub>2</sub> electrode observed in this study could be due to the amount of organic components used to prepare the initial paste. Park et al.<sup>18</sup> reported on pastes prepared with an acetic acid:Ti ratio of approximately 10:1 compared with the ratio of 1:1 used in the present work. As the FTIR results suggested [Fig. 4(b)], the processing conditions of films at 150 °C for 15 min are not sufficient enough to eliminate all the organics from the TiO<sub>2</sub> film. The presence of organics is expected to limit the electron diffusion through the cell and thus decrease the DSSC performance efficiency.

The presence of organics in the TiO<sub>2</sub> electrode and its effect on the DSSC performance were further investigated by varying the thermal treatment conditions. Electrodes were either air dried or heat treated for periods up to 24 h, which clearly resulted in reduced amount of organics retained in the structure, as observed by the FTIR [Fig. 4(d)]. This observation in turn translated to a corresponding increase in  $I_{SC}$  and in efficiency conversion efficiencies from 7.78 to 9.86 mA/cm<sup>2</sup> and 4.10% to 5.44%, respectively (Table II, entries 3, 7–9).

TABLE II. Photovoltaic performance of dye-sensitized solar cells based on the 1-TiO<sub>2</sub> paste.

Entry	Thickness, $\mu\text{m}$	Post-treatment	$V_{OC}$ , mV	$I_{SC}$ , mA/cm <sup>2</sup>	FF	$\eta$ , %
1	2.5		783	7.39	0.73	4.23
2	3.0		773	8.80	0.73	4.96
3	4.2	15 min at 150 °C	775	8.83	0.73	5.00
4	5.9		760	8.14	0.73	4.50
5	6.2		765	8.51	0.74	4.80
6	7.7		775	6.11	0.72	3.48
7	4.2	Air dried	763	7.78	0.69	4.10
8	4.2	2 h at 150 °C	780	9.10	0.72	5.07
9	4.2	24 h at 150 °C	763	9.86	0.73	5.44
10	4.1	30 min at 450 °C	760	11.36	0.70	6.00

Moreover, thermal treatment to 450 °C for 30 min (Table II, entry 8) produced further increases in  $I_{SC}$  and energy conversion efficiency values ( $I_{SC} = 11.36 \text{ mA/cm}^2$  and  $\eta = 6\%$ ), where it is known that the organic has been completely removed [Fig. 4(e)] within the electrode microstructure. This result demonstrates the versatility of this formulation in the preparation of both low and high temperature electrodes for DSSC devices.

A mechanism for TiO<sub>2</sub> interparticle connectivity with thermal treatment at 150 °C is proposed in Fig. 5. In contrast to sintering electrodes at 450 °C, where TiO<sub>2</sub> particles bind via necking,<sup>31</sup> particles treated at 150 °C relied on the formation Ti–O–Ti bridges formed by dehydration of surface hydroxyls.<sup>32</sup>

Figure 6 illustrates the efficiency of TiO<sub>2</sub> electrodes prepared as a function of film thickness. For the TiO<sub>2</sub> films produced with equivalent thermal treatment, the efficiency increased slightly with the increase in film thickness and reaches maximum value of 5% for the 4.2  $\mu\text{m}$  film. It then decreased gradually to approximately 3.48% for the 7.7  $\mu\text{m}$  thick TiO<sub>2</sub> film.

Finally, we have conducted some preliminary experiments measuring the photovoltaic performance of the DSSC devices prepared from TiO<sub>2</sub> pastes aged between 1 and 9 months. TiO<sub>2</sub> suspension stability is considered an important technological issue in the storage of pastes. To investigate the effect of aging on performance, films with a thickness of 4.5  $\mu\text{m}$  were prepared from pastes aged after 4 and 9 months, respectively, and compared to paste prepared within a month. Performance data show no more than 4% deviation in  $I_{SC}$  corresponding to approximately 5% drop in the overall energy conversion efficiency

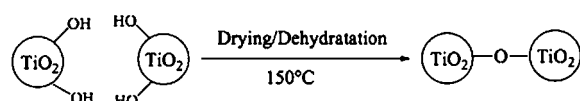


FIG. 5. A mechanism for TiO<sub>2</sub> particles interconnection via a dehydration step occurring within the film at 150 °C.

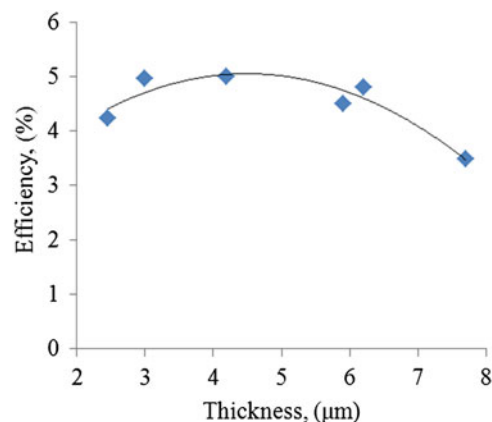


FIG. 6. Efficiency of TiO<sub>2</sub> electrodes as a function of film thickness.



To further investigate the performance of TiO<sub>2</sub> electrodes, EIS measurements were undertaken to determine the effect of TiO<sub>2</sub> electrode thickness and thermal treatment on device efficiency. Figure 7 shows Nyquist (a, b) and Bode (c, d) plots for cells with different TiO<sub>2</sub> thicknesses (a, c) and thermal treatment (b, d). An arc in the Nyquist plot represents existence of electrochemical interfaces. In increasing the order of frequency, these semicircles are attributed to the Nerstian diffusion within the electrolyte, the electron transfer at the oxide/electrolyte interface, and the redox reaction at the platinum counter electrode.<sup>33</sup> A distinct change in both plots appeared between electrodes samples based on film thickness and thermal treatment. All semicircles observed on Fig. 7(a) expanded slightly when the TiO<sub>2</sub> film thickness increased. Moreover, the border between arcs of higher (~400–1 kHz) and lower frequency (~1 kHz to 10 Hz) became featureless indicating a diminished electrical contact between TiO<sub>2</sub> nanoparticles in the device. Similar results were observed by Hoshikawa et al.,<sup>34</sup> who investigated different temperatures in the sintering process of TiO<sub>2</sub> particles. They concluded that at lower process temperatures, there were many more grain boundaries, which remained

between TiO<sub>2</sub> particles and prevented efficient electron transport.

To gain a better insight about electron transport through nanocrystalline TiO<sub>2</sub> electrode, the electron lifetimes were estimated from the Bode plots [Fig. 7(b)]. Electron lifetimes were calculated from the phase shift versus frequency plots as  $1/\omega_{\min}$ , where  $\omega_{\min}$  is the frequency at which the phase shift is minimum. The calculated values of electron lifetimes ( $\tau$ ) for the TiO<sub>2</sub> thicknesses of 3, 4.2, and 5.9  $\mu\text{m}$  were 1.3, 1.0, and 0.06 ms, respectively. The decreased electron lifetime with greater TiO<sub>2</sub> electrode thickness suggests a reduction in electron diffusion through the TiO<sub>2</sub> layer, which ultimately affected the device performance<sup>35</sup> as reported in the Sec. III. D.

The appearance of two distinct semicircles in Nyquist plot [Fig. 7(c)] with increasing thermal treatment time (from 15 min to 24 h) suggests an improvement in particle interconnectivity within the network, which is consistent with SEM and N<sub>2</sub> sorption analysis discussed previously. Moreover, an increase of electron lifetimes from 1.0 to 1.6 ms with thermal treatment time was also calculated according to Bode plots [Fig. 7(d)]. This result suggests

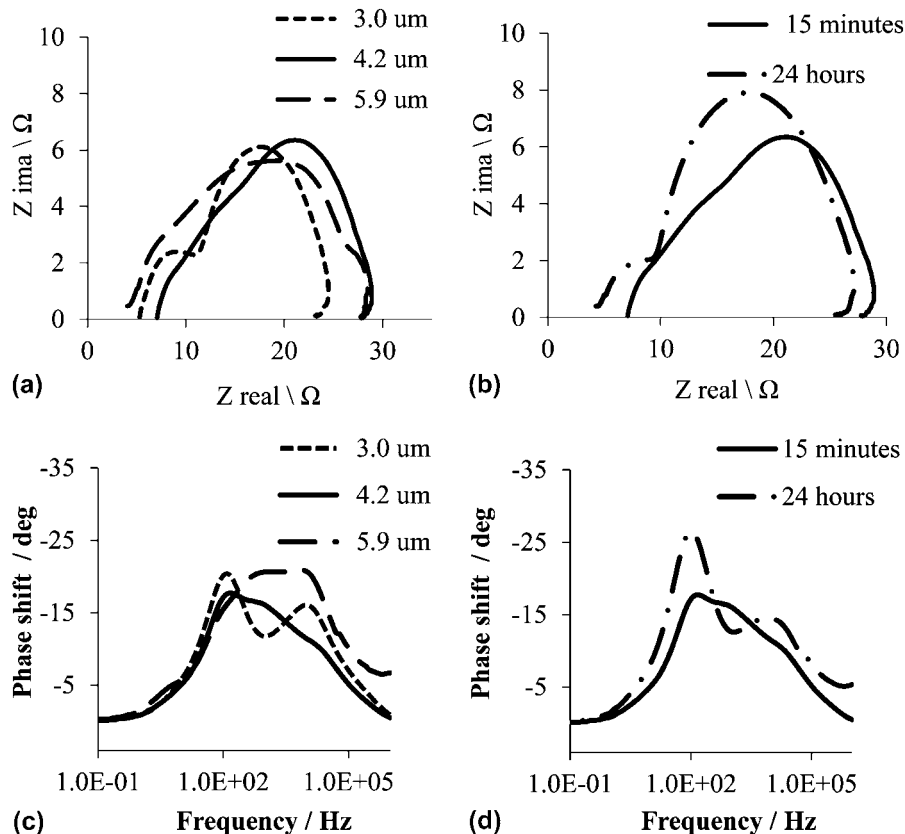


FIG. 7. The Nyquist plots of (a) thermal treated at 150 °C for 15 min for different films thickness; (b) 4.2- $\mu\text{m}$ -thick films at different post-treatment and Bode diagrams of (c) thermal treated at 150 °C for 15 min for different films thickness; (d) 4.2- $\mu\text{m}$ -thick films at different thermal treatment; the electrochemical impedance spectra.

less electron recombination induced by the presence of electron traps from residual organics.

#### IV. CONCLUSIONS

This study has addressed one of the key challenges for the preparation of low temperature DSSCs, which is to prepare films with good TiO<sub>2</sub> particle interconnectivity and low residual organic content to maximize electron transport. Chemical modification of TiO<sub>2</sub> suspensions can serve to provide viscous paste for the preparation of robust electrodes for low temperature processing. The influence of ammonia on paste rheology was investigated and found that changes occurred due to particle flocculation in the slurry. The suspension was stable for at least 9 months, the duration of this study, yielding continuous and uniform thick films. The presence of organics within the TiO<sub>2</sub> electrode was probed by FTIR, and acetate ligands were found to remain in the structure after thermal treatment at 150 °C for 24 h. Modifying the TiO<sub>2</sub> precursor in the preparation of a colloidal suspension with a 10-fold decrease in acetic acid ensured that minimal quantities of acetate ligands were present in the TiO<sub>2</sub> electrode. This starting TiO<sub>2</sub> precursor led to improvements in energy conversion efficiency of approximately 75% to produce devices with  $\eta > 5\%$  without the need to heat treat at temperatures  $> 150$  °C.

#### ACKNOWLEDGMENTS

This research was carried out under funding provided by the Cooperative Research Centre for Polymers III. The authors wish to thank Dr. Ian Dagley (CEO) and the participants of Project 3.1. In particular, the authors also wish to thank Dr. Rohan Holmes for his assistance with rheology measurements and Dr. Peter Evans for fruitful discussions.

#### REFERENCES

1. B. O'Regan and M. Grätzel: A low-cost, high-efficiency solar cell based on dye-sensitized colloidal TiO<sub>2</sub> films. *Nature* **353**, 737 (1991).
2. A. Yella, H.W. Lee, H.N. Tsao, C.Y. Yi, A.K. Chandiran, M.K. Nazeeruddin, E.W.G. Diau, C.Y. Yeh, S.M. Nazeeruddin, and M. Grätzel: Porphyrin-sensitized solar cells with cobalt (II/III)-based redox electrolyte exceed 12 percent efficiency. *Science* **334**(6056), 629 (2011).
3. S. Ito, T.N. Murakami, P. Comte, P. Liska, C. Grätzel, M.K. Nazeeruddin, and M. Grätzel: Fabrication of thin film dye sensitized solar cells with solar to electric power conversion efficiency over 10%. *Thin Solid Films* **516**(14), 4613 (2008).
4. H. Lindstrom, A. Holmberg, E. Magnusson, L. Malmqvist, and A. Hagfeldt: A new method to make dye-sensitized nanocrystalline solar cells at room temperature. *J. Photochem. Photobiol., A* **145**(1–2), 107 (2001).
5. A. Hagfeldt, G. Boschloo, H. Lindstrom, E. Figgemeier, A. Holmberg, V. Aramios, E. Magnusson, and L. Malmqvist: A system approach to molecular solar cells. *Coord. Chem. Rev.* **248** (13–14), 1501 (2004).
6. T. Yamaguchi, N. Tobe, D. Matsumoto, and H. Arakawa: Highly efficient plastic substrate dye-sensitized solar cells using a compression method for preparation of TiO<sub>2</sub> photoelectrodes. *Chem. Commun.* 4767 (2007).
7. T. Yamaguchi, N. Tobe, D. Matsumoto, and H. Arakawa: Highly efficient plastic-substrate dye-sensitized solar cells with validated conversion efficiency of 7.6%. *Sol. Energy Mater. Sol. Cells* **94**(5), 812 (2010).
8. G. Boschloo, J. Lindstrom, E. Magnusson, A. Holmberg, and A. Hagfeldt: Optimization of dye-sensitized solar cells prepared by compression method. *J. Photochem. Photobiol., A* **148**(1–3), 11 (2002).
9. H.C. Weerasinghe, P.M. Sirimanne, G.P. Simon, and Y-B. Cheng: Cold isostatic pressing technique for producing highly efficient flexible dye-sensitized solar cells on plastic substrates. *Prog. Photovoltaics Res. Appl.* **20**(3), 321 (2012).
10. D. Zhang, T. Yoshida, and H. Minoura: Low temperature synthesis of porous nanocrystalline TiO<sub>2</sub> thick film for dye-sensitized solar cells by hydrothermal crystallization. *Chem. Lett.* **31**(9), 874 (2002).
11. D. Zhang, T. Yoshida, and H. Minoura: Low-temperature fabrication of efficient porous titania photoelectrodes by hydrothermal crystallization at the solid/gas interface. *Adv. Mat.* **15**(10), 814 (2003).
12. D. Zhang, T. Yoshida, K. Furuta, and H. Minoura: Hydrothermal preparation of porous nano-crystalline TiO<sub>2</sub> electrodes for flexible solar cells. *J. Photochem. Photobiol., A* **164**(1–3), 159 (2004).
13. T.N. Murakami, Y. Kijitori, N. Kawashima, and T. Miyasaka: Low temperature preparation of mesoporous TiO<sub>2</sub> films for efficient dye-sensitized photoelectrode by chemical vapor deposition combined with UV light irradiation. *J. Photochem. Photobiol., A* **164**(1–3), 187 (2004).
14. D. Zhang, T. Yoshida, T. Oekermann, K. Furuta, and H. Minoura: Room-temperature synthesis of porous nanoparticulate TiO<sub>2</sub> films for flexible dye-sensitized solar cells. *Adv. Funct. Mat.* **16**(9), 1228 (2006).
15. L.N. Lewis, J.L. Spivack, S. Gasaway, E.D. Williams, J.Y. Gui, V. Manivannan, and O.P. Siclován: A novel UV-mediated low-temperature sintering of TiO<sub>2</sub> for dye-sensitized solar cells. *Sol. Energy Mater. Sol. Cells* **90**(7–8), 1041–1051 (2006).
16. S. Uchida, M. Tomiha, H. Takizawa, and M. Kawayara: Flexible dye-sensitized solar cells by 28 GHz microwave irradiation. *J. Photochem. Photobiol., A* **164**(1–3), 93 (2004).
17. D.B. Menzies, Q. Dai, Y-B. Cheng, G.P. Simon, and L. Spiccia: One-step microwave calcination of ZrO<sub>2</sub>-coated TiO<sub>2</sub> electrodes for use in dye-sensitized solar cells. *C.R. Chim.* **9**(5–6), 713 (2006).
18. N.G. Park, K.M. Kim, M.G. Kang, K.S. Ryu, S.H. Chang, and Y.J. Shin: Chemical sintering of nanoparticles: A methodology for low-temperature fabrication of dye-sensitized TiO<sub>2</sub> films. *Adv. Mater.* **17**(19), 2349 (2005).
19. K. Kim, G.W. Lee, K. Yoo, D.Y. Kim, J.K. Kim, and N.G. Park: Improvement of electron transport by low-temperature chemically assisted sintering in dye-sensitized solar cell. *J. Photochem. Photobiol., A* **204**(2–3), 144 (2009).
20. P. Zhang, C. Wu, Y. Han, T. Jin, B. Chi, J. Pu, and L. Jian: Low-temperature preparation of hierarchical structure TiO<sub>2</sub> for flexible dye-sensitized solar cell. *J. Am. Ceram. Soc.* **95**(4), 1 (2012).
21. H.C. Weerasinghe, G.V. Franks, J.D. Plessis, G.P. Simon, and Y-B. Cheng: Anomalous rheological behavior in chemically modified TiO<sub>2</sub> colloidal pastes prepared for flexible dye-sensitized solar cells. *J. Mater. Chem.* **20**(44), 9954 (2010).
22. H.C. Weerasinghe, P.M. Sirimanne, G.V. Franks, G.P. Simon, and Y-B. Cheng: Low temperature chemically sintered nano-crystalline

- TiO<sub>2</sub> electrodes for flexible dye-sensitized solar cells. *J. Photochem. Photobiol., A* **213**(1), 30 (2010).
23. I. Karatchevtseva, D.J. Cassidy, Z.M. Zhang, G. Triani, K.S. Finnie, S.L. Cram, and C.J. Barbe: Crystallization of TiO<sub>2</sub> powders and thin films prepared from modified titanium alkoxide precursors. *J. Am. Ceram. Soc.* **91**(6), 2015 (2008).
24. T.X. Liu, F.B. Li, and X.Z. Li: Effects of peptizing conditions on nanometer properties and photocatalytic activity of TiO<sub>2</sub> hydrosols prepared by H<sub>2</sub>TiO<sub>3</sub>. *J. Hazard. Mater.* **155**(1–2), 90 (2008).
25. S. Winardi, R.R. Mukti, K.N.P. Kumar, J.Z. Wang, W. Wunderlich, and T. Okubo: Critical nuclei size, initial particle size and packing effect on the phase stability of sol-peptization-gel-derived nanostructured titania. *Langmuir* **26**(7), 4567 (2010).
26. S. Ito, M.K. Nazeeruddin, P. Liska, P. Comte, R. Charvet, P. Pechy, M. Jirousek, A. Kay, S.M. Zakeeruddin, and M. Grätzel: Photo-voltaic characterization of dye-sensitized solar cells: Effect of device masking on conversion efficiency. *Prog. Photovoltaics Res. Appl.* **14**, 589 (2006).
27. S. Doeuff, M. Henry, C. Sanchez, and J. Livage: Hydrolysis of titanium alkoxides: Modification of the molecular precursor by acetic acid. *J. Non-Cryst. Solids* **89**(1–2), 206–216 (1987).
28. S.K. Dhungel and J.G. Park: Optimization of paste formulation for TiO<sub>2</sub> nanoparticles with wide range of size distribution for its application in dye sensitized solar cells. *Renew. Energy* **35**(12), 2776 (2010).
29. K.S.W. Sing, D.H. Everett, R.A.W. Haul, L. Moscou, R.A. Pierotti, J. Rouquerol, and T. Siemieniwska: Reporting physisorption data for gas/solid systems with special reference to the determination of surface area and porosity. *Pure Appl. Chem.* **57**(4), 603 (1985)
30. G. Socrates: *Infrared and Raman Characteristic Group Frequencies: Tables and Charts*, 3rd ed. (Wiley & Sons, Ltd., Chichester, UK, 2001), p. 128.
31. P.T. Hsiao and H.S. Teng: Coordination of Ti<sup>4+</sup> sites in nano-crystalline TiO<sub>2</sub> films used for photoinduced electron conduction: Influence of nanoparticle synthesis and thermal necking. *J. Am. Ceram. Soc.* **92**(4), 888–893 (2009).
32. T. Miyasaka, M. Ikegami, and Y. Kijitori: Photovoltaic performance of plastic dye-sensitized electrodes prepared by low-temperature binder-free coating of mesoscopic titania. *J. Electrochem. Soc.* **154**(5), A455 (2007).
33. Q. Wang, J.E. Moser, and M. Grätzel: Electrochemical impedance spectroscopic analysis of dye-sensitized solar cells. *J. Phys. Chem. B* **109**, 14945 (2005).
34. T.T. Hoshikawa, M. Yamada, R. Kikuchi, and K. Eguchi: Impedance analysis for dye-sensitized solar cells with a three-electrode system. *J. Electrochem. Soc.* **152**, E68 (2005).
35. C.P. Hsu, K.M. Lee, J.T.W. Huang, C.Y. Lin, C.H. Lee, L.P. Wang, S.Y. Tsai, and K.C. Ho: EIS analysis on low temperature fabrication of TiO<sub>2</sub> porous films for dye-sensitized solar cells. *Electrochim. Acta* **53**, 7514 (2008).

### Supplementary Material

Supplementary material can be viewed in this issue of the *Journal of Materials Research* by visiting <http://journals.cambridge.org/jmr>.